Supplementary Information for

Mass Spectrometry Imaging Disclosed Spatial Distribution of Defense-Related Metabolites in *Triticum* spp.

Laura Righetti [1,2,*], Sven Gottwald [1], Sara Tortorella [3], Bernhard Spengler [1] and Dhaka Ram Bhandari [1,4,*]

[1] Institute of Inorganic and Analytical Chemistry, Justus Liebig University Giessen, Heinrich-Buff-Ring 17, 35392 Giessen, Germany; sv.gottwald@t-online.de (S.G.); bernhard.spengler@anorg.chemie.uni-giessen.de (B.S.)
[2] Food and Drug Department, University of Parma, Viale delle Scienze 17/A, 43124 Parma, Italy
[3] Molecular Horizon Srl., Via Montelino 30, Bettona, 06084 Perugia, Italy; sara@molhorizon.it
[4] Gandaki Prvince Academy of Science and Technology, Pokhara 33700, Nepal
* Correspondence: laura.righetti@unipr.it (L.R.); dhaka.r.bhandari@transmit.de (D.R.B.)

Table S1. List of metabolites imaged in common and durum wheat and differentially accumulated in non-infected vs infected kernels. The reference column gives cited references for metabolites detected in previous studies on wheat or other plants. The citation details are provided in the reference list.

Subclass	Putative identification	Formula	Adduct	Detected *m/z*	Infected kernel	Non-infected kernel	Ref
N-acyl amines	Hydroxyhexadecadienoylcarnitine	$C_{23}H_{41}NO_5$	$[M+H]^+$	412.3057	Endosperm and aleurone	N.D.	[1]
	Hydroxy-hexadecenoylcarnitine	$C_{23}H_{43}NO_5$	$[M+H]^+$	414.3214	Endosperm and aleurone	N.D.	[1]
	Hexadecanedioic acid mono-carnitine ester	$C_{23}H_{43}NO_6$	$[M+H]^+$	430.3163	Endosperm and aleurone	N.D.	[1]
Unsaturated fatty acid	Alpha-Linolenic acid	$C_{18}H_{30}O_2$	$[M+H]^+$	279.2318	Endosperm	N.D.	[2]
	12,13-EOTrE	$C_{18}H_{28}O_3$	$[M+H]^+$	293.2111	Endosperm	N.D.	[3]
	Linoleic acid	$C_{18}H_{32}O_2$	$[M+K]^+$	319.2033	Endosperm	N.D.	[2]
	13-HOME	$C_{18}H_{34}O_3$	$[M+Na]^+$	321.2400	Endosperm	N.D.	[4]
	13-OxoODE	$C_{18}H_{30}O_3$	$[M+K]^+$	333.1826	Endosperm	N.D.	[3]
	13-HODE	$C_{18}H_{32}O_3$	$[M+K]^+$	335.1983	Endosperm	N.D.	[4]
	13-HpOTrE	$C_{18}H_{30}O_4$	$[M+K]^+$	349.1775	Endosperm	N.D.	[5]
	13-HpODE/ 12,13-DiHODE	$C_{18}H_{32}O_4$	$[M+K]^+$	351.1932	Endosperm	N.D.	[3]
	12,13-diHOME	$C_{18}H_{34}O_4$	$[M+K]^+$	353.2088	Endosperm	N.D.	[5]
	2-HpOTrE	$C_{18}H_{30}O_5$	$[M+K]^+$	365.1724	Endosperm	N.D.	
	TriHODE/ 9,10-Dihydroxy-8-oxo-12-octadecenoic acid	$C_{18}H_{32}O_5$	$[M+K]^+$	367.1881	Endosperm	N.D.	[5]
	TriHOME	$C_{18}H_{34}O_5$	$[M+K]^+$	369.2037	Endosperm	N.D.	[5]
Sterol	ergosterol	$C_{28}H_{44}O$	$[M+H-H_2O]^+$	379.3359	Endosperm	N.D.	[6]
			$[M+H]^+$	397.3465	Endosperm	N.D.	[6]
Vitamin D3 and derivatives	Hydroxy-oxo-hexanorvitamin D3	$C_{21}H_{30}O_3$	$[M+Na]^+$	353.2087	Endosperm	N.D.	[7]
	Dihydroxy-oxo-hexanorvitamin D3	$C_{21}H_{30}O_4$	$[M+Na]^+$	369.2036	Endosperm	N.D.	[7]
	Vitamin D3/7-Dehydrocholesterol	$C_{27}H_{44}O$	$[M+K]^+$	423.3023	Endosperm	N.D.	[7]
	Dihydroxy-epivitamin D3	$C_{27}H_{44}O_3$	$[M+K]^+$	455.2922	Endosperm	N.D.	[7]
	Trihydroxyvitamin D3	$C_{27}H_{44}O_4$	$[M+K]^+$	471.2871	Endosperm	N.D.	[7]

	Tetrahydroxyvitamin D3	$C_{27}H_{44}O_5$	$[M+K]^+$	487.2820	Endosperm	N.D.	[7]
	Dihydroxyl-didehydro-trihomovitamin D3	$C_{30}H_{48}O_3$	$[M+K]^+$	495.3235	Endosperm	N.D.	[7]
	Diethyl-dihydroxyl-didehydro-oxavitamin D3	$C_{30}H_{48}O_4$	$[M+K]^+$	511.3184	Endosperm	N.D.	[7]
Carbohydrates and carbohydrate conjugates	Tetra-hexose	$C_{24}H_{40}O_{20}$	$[M+K]^+$	687.1744	Endosperm	N.D.	[8]
	Apiosylglucosyl hydroxybenzoate	$C_{18}H_{24}O_{12}$	$[M+Na]^+$	455.1160	Endosperm	N.D.	[8]
Triterpenoids	Feruloylcorosocolic acid	$C_{40}H_{56}O_7$	$[M+H]^+$	649.4099	Pericarp and testa	N.D.	
	Gibbeellin glucosyl ester	$C_{25}H_{34}O_{11}$	$[M+H]^+$	511.2174	Pericarp and testa	N.D.	
	Methyl-apocarotenoate	$C_{33}H_{44}O_2$	$[M+Na]^+$	495.3233	Endosperm and aleurone	N.D.	
Phenolic glycosides	Flavonoid glycoside	$C_{34}H_{40}O_{22}$	$[M+Na]^+$	823.1903	Endosperm	N.D.	[9]
	Kaempferol rhamnoside	$C_{35}H_{42}O_{20}$	$[M+K]^+$	821.1901	Pericarp	N.D.	
	Methyl liquiritugenin rhamnoside	$C_{22}H_{24}O_8$	$[M+H]^+$	417.1544	Pericarp	N.D.	
Quinone and hydroquinone lipids	Vit D2 hydroquinone	$C_{21}H_{26}O_2$	$[M+Na]^+$	333.1825	Endosperm	N.D.	
Purine 2'-deoxyribonucleosides	Hydroxy-deoxyguanosine	$C_{10}H_{13}N_5O_5$	$[M+K]^+$	322.0548	Endosperm	N.D.	[10]
Carbonyl compounds	Falcarindione	$C_{17}H_{20}O_2$	$[M+H]^+$	257.1536	Pericarp and VB	N.D.	[11]
Simple Glc series	GlcCer (d14:1/20:0(OH))	$C_{40}H_{77}NO_9$	$[M+K]^+$	754.5230	Endosperm	N.D.	[5]
Glycerophosphates	PA (42:8)	$C_{45}H_{73}O_8P$	$[M+K]^+$	811.4674	Pericarp	N.D.	
Diacylglycerols	DG (36:8)	$C_{39}H_{60}O_5$	$[M+Na]^+$	631.4333	Pericarp	N.D.	[4]
Glycerophospholipids	PC(24:2) /PE-NMe(36:2)	$C_{42}H_{80}NO_8P$	$[M+H]^+$	758.5694	N.D.	Endosperm	
			$[M+Na]^+$	780.5513	N.D.	Endosperm	
	PC (24:1)/PE-NMe(36:1)	$C_{42}H_{82}NO_8P$	$[M+H]^+$	760.5850	N.D.	Endosperm	
	PE (20:4/P-18:1)	$C_{43}H_{76}NO_7P$	$[M+Na]^+$	772.5251	N.D.	Endosperm	
	PC (32:0), PE(35:0), PE-NMe(34:0)	$C_{40}H_{80}NO_8P$	$[M+K]^+$	772.5253	N.D.	Endosperm	
	PC (26:4)/ PE-NMe(38:4)	$C_{44}H_{80}NO_8P$	$[M+H]^+$	782.5694	N.D.	Endosperm	
	PE (22:6/P-18:1)	$C_{45}H_{76}NO_7P$	$[M+Na]^+$	796.5251	N.D.	Aleurone and endosperm	
	PG (40:6)	$C_{46}H_{79}O_{10}P$	$[M+H]^+$	823.5448	N.D.	Aleurone	
	PG (36:2)	$C_{42}H_{79}O_{10}P$	$[M+Na]^+$	797.5303	N.D.	Endosperm	
	PE (22:5/P-18:1)	$C_{45}H_{78}NO_7P$	$[M+Na]^+$	798.5408	N.D.	Aleurone and endosperm	

	PS (46:7)	$C_{52}H_{88}NO_{10}P$	$[M+K]^+$	956.5777	N.D.	Endosperm	
	LysoPC (16:0)	$C_{24}H_{50}NO_7P$	$[M+Na]^+$	518.3217	N.D.	Endosperm	
Glycosylglycerols	MGDG (34:2)	$C_{43}H_{78}O_{10}$	$[M+K]^+$	793.5226	N.D.	Endosperm	[12]
	DGDG (36:9)	$C_{51}H_{78}O_{15}$	$[M+K]^+$	795.5383	N.D.	Endosperm	[12]
	MGDG (36:9)	$C_{45}H_{68}O_{10}$	$[M+K]^+$	796.5410	N.D.	Endosperm	[12]
	Glycerol -(octadecadienoate) -hexadecanoate-[galactopyranosyl-galactopyranoside]	$C_{49}H_{88}O_{15}$	$[M+Na]^+$	939.6015	N.D.	Endosperm	

- **Linoleic acid metabolism**

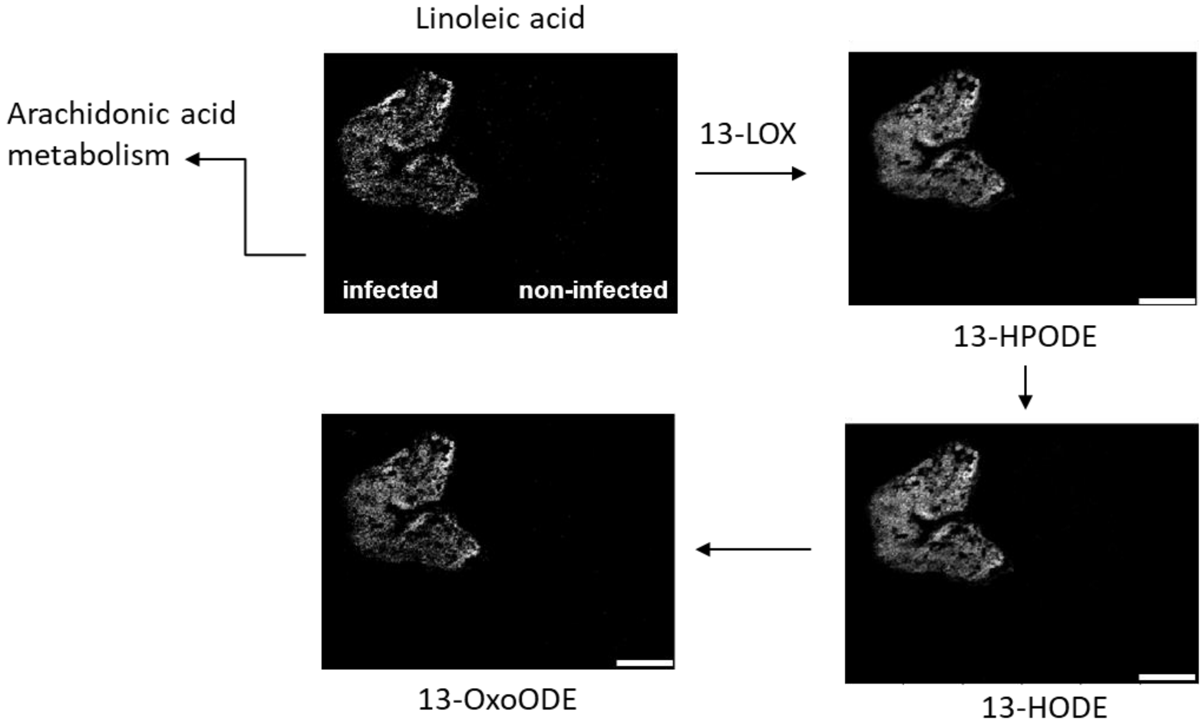

Figure S1. Spatial distribution of linoleic acid and oxylipins in common-wheat cross-sections: linoleic acid $[M+K]^+$ *m/z* 319.2034, 13-HPODE $[M+K]^+$ *m/z* 351.1932, 13-HODE $[M+K]^+$ *m/z* 335.1983, 13-oxoODE $[M+K]^+$ *m/z* 333.1826.
MS images were generated with 300 x 220 pixels; 15 µm pixel size; *m/z* bin width: ± 5 ppm; Scale bars: 400 µm.

- **α-Linoleic acid metabolism**

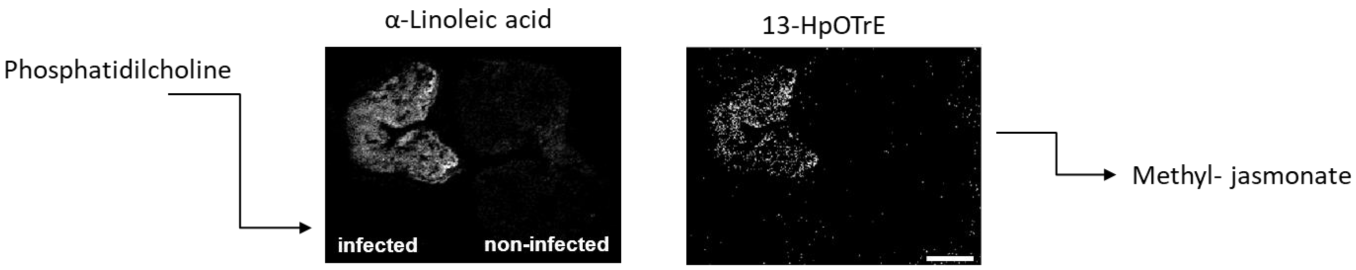

Figure S2. Spatial distribution of α-linoleic acid $[M+H]^+$ *m/z* 279.2318 and 13-HpOTrE $[M+K]^+$ *m/z* 349.1775 in common-wheat cross-sections.
MS images were generated with 300 x 220 pixels; 15 µm pixel size; *m/z* bin width: ± 5 ppm;. Scale bars: 400 µm.

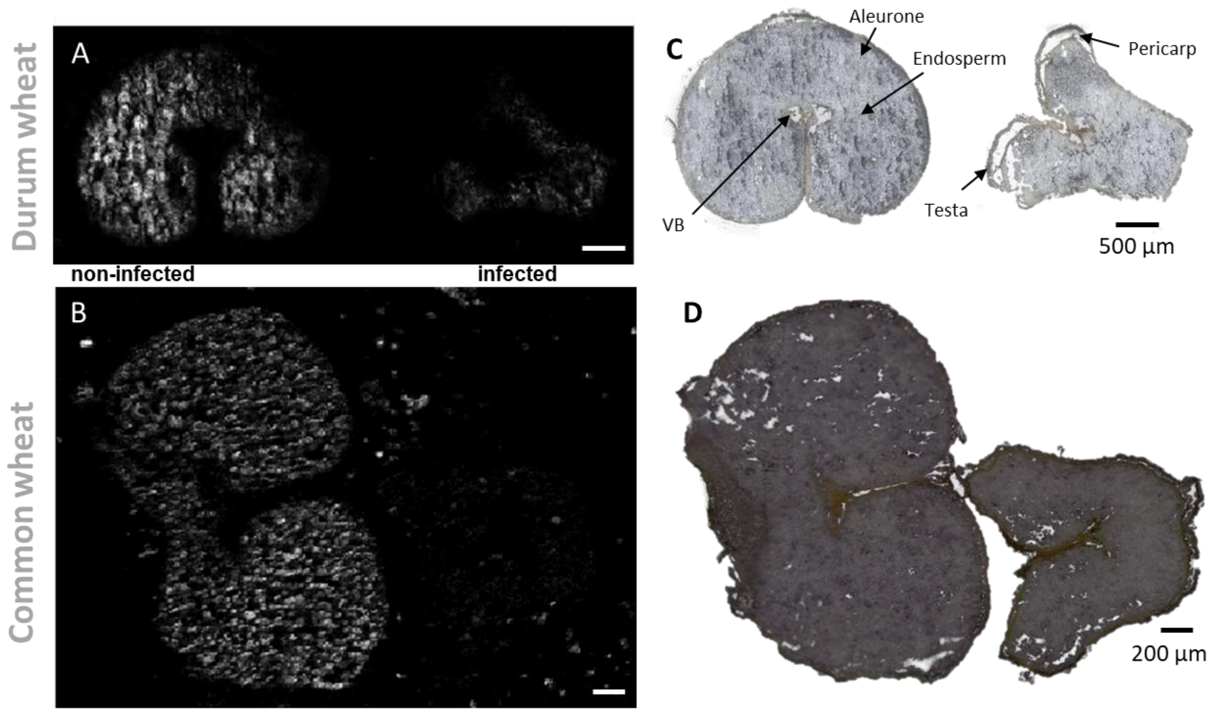

Figure S3. Spatial distribution of lyso-phosphatidylcholine in durum- (A) and common-wheat (B) cross-sections. LysoPC (16:0) $[M+Na]^+$ *m/z* 518.3216 was found accumulated mainly in the endosperm of the non-infected seed. Optical image of durum- (C) and common-wheat (D) seed section with major morphological features labeled.

MS images were generated with (A) 336 x 138 pixels; 20 µm pixel size; *m/z* bin width: ± 5 ppm; scale bars: 500 µm; (B) 300 x 220 pixels; 15 µm pixel size; *m/z* bin width: ± 5 ppm; scale bars: 200 µm.

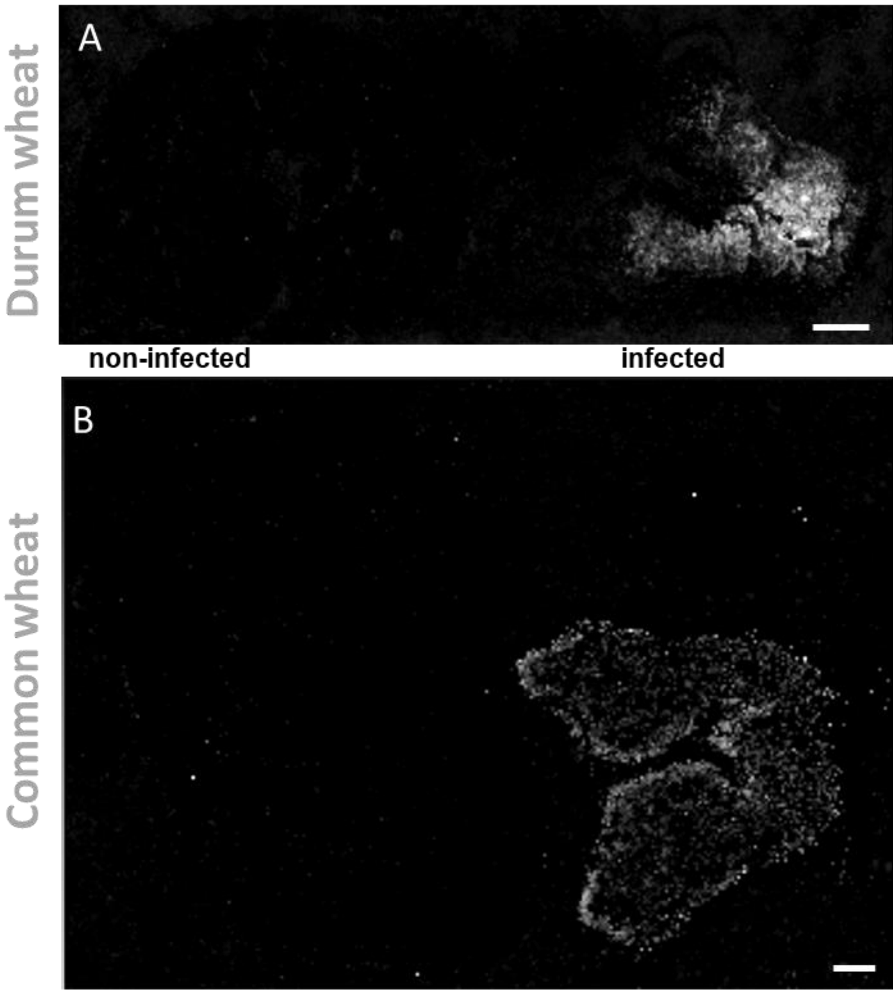

Figure S4. Spatial distribution of carbohydrates in durum- (A) and common-wheat (B) cross-sections. Trisaccharide $[M+K]^+$ *m/z* 513.1222 was found accumulated exclusively in the infected seed.

MS images were generated with (A) 336 x 138 pixels; 20 µm pixel size; *m/z* bin width: ± 5 ppm; scale bars: 500 µm; (B) 300 x 220 pixels; 15 µm pixel size; *m/z* bin width: ± 5 ppm; scale bars: 200 µm.

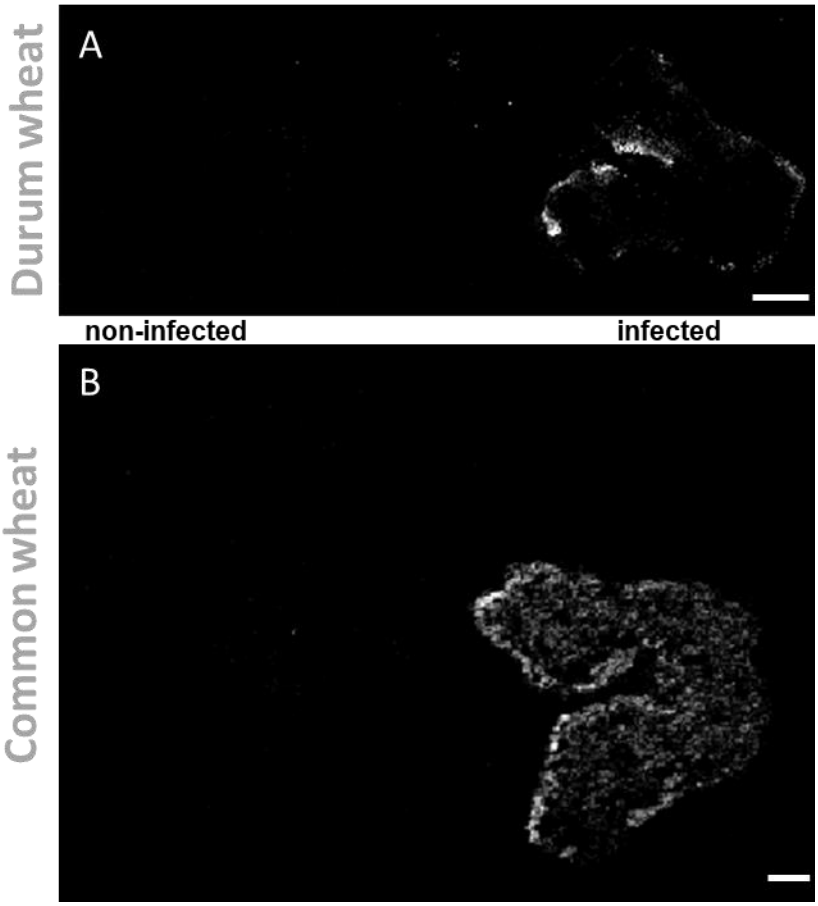

Figure S5. Spatial distribution of N-acyl amines in durum- (A) and common-wheat (B) cross-sections. Hydroxy-hexadecadienoylcarnitine $[M+H]^+$ *m/z* 412.3057 was found accumulated exclusively in the infected seed.

MS images were generated with (A) 336 x 138 pixels; 20 µm pixel size; *m/z* bin width: ± 5 ppm; scale bars: 500 µm; (B) 300 x 220 pixels; 15 µm pixel size; *m/z* bin width: ± 5 ppm; scale bars: 200 µm.

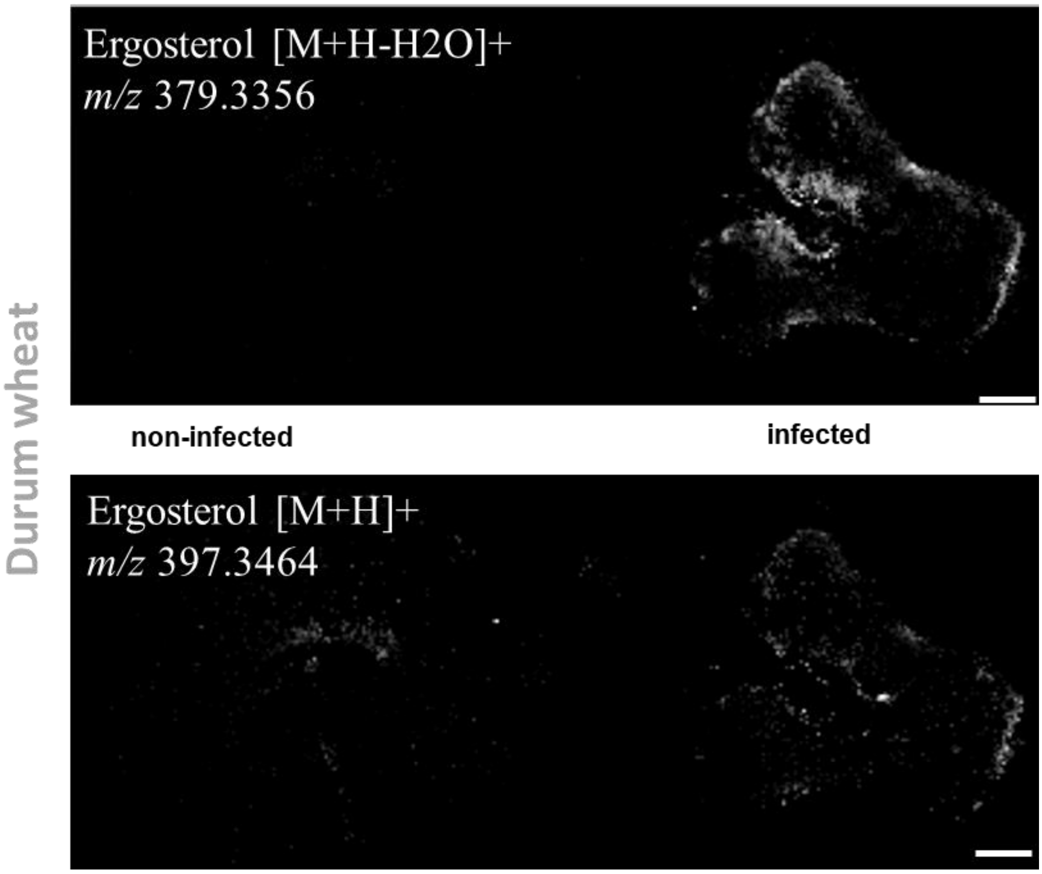

Figure S6. Spatial distribution of ergosterol in durum-wheat cross-sections. The $[M+H]^+$ image was normalized to the total ion count on a 0-60% intensity scale.

MS images were generated with 336 x 138 pixels; 20 µm pixel size; *m/z* bin width: ± 5 ppm; scale bars: 500 µm.

References

1. Bhandari, D.R.; Wang, Q.; Friedt, W.; Spengler, B.; Gottwald, S.; Römpp, A. High resolution mass spectrometry imaging of plant tissues: towards a plant metabolite atlas. *Analyst* **2015**, *140*, 7696–7709, doi:10.1039/C5AN01065A.

2. Righetti, L.; Lucini, L.; Giorni, P.; Locatelli, S.; Dall'Asta, C.; Battilani, P. Lipids as Key Markers in Maize Response to Fumonisin Accumulation. *J. Agric. Food Chem.* **2019**, *67*, 4064–4070, doi:10.1021/acs.jafc.8b06316.

3. Tsitsigiannis, D.I.; Keller, N.P. Oxylipins as developmental and host-fungal communication signals. *Trends Microbiol.* 2007, *15*.

4. Rubert, J.; Righetti, L.; Stranska-Zachariasova, M.; Dzuman, Z.; Chrpova, J.; Dall'Asta, C.; Hajslova, J. Untargeted metabolomics based on ultra-high-performance liquid chromatography–high-resolution mass spectrometry merged with chemometrics: A new predictable tool for an early detection of mycotoxins. *Food Chem.* **2017**, *224*, 423–431, doi:10.1016/j.foodchem.2016.11.132.

5. Scala, V.; Giorni, P.; Cirlini, M.; Ludovici, M.; Visentin, I.; Cardinale, F.; Fabbri, A.A.; Fanelli, C.; Reverberi, M.; Battilani, P.; et al. LDS1-produced oxylipins are negative regulators of growth, conidiation and fumonisin synthesis in the fungal maize pathogen Fusarium verticillioides. *Front. Microbiol.* **2014**, *5*, doi:10.3389/fmicb.2014.00669.

6. Varga, M.; Bartók, T.; Mesterházy, Á. Determination of ergosterol in Fusarium-infected wheat by liquid chromatography-atmospheric pressure photoionization mass spectrometry. *J. Chromatogr. A* **2006**, *1103*, doi:10.1016/j.chroma.2005.11.051.

7. Jäpelt, R.B.; Jakobsen, J. Vitamin D in plants: A review of occurrence, analysis, and biosynthesis. *Front. Plant Sci.* 2013, *4*.

8. Gauthier, L.; Atanasova-Penichon, V.; Chéreau, S.; Richard-Forget, F. Metabolomics to Decipher the Chemical Defense of Cereals against Fusarium graminearum and Deoxynivalenol Accumulation. *OPEN ACCESS Int. J. Mol. Sci* **2015**, *16*, 16, doi:10.3390/ijms161024839.

9. Bhandari, D.R.; Wang, Q.; Li, B.; Friedt, W.; Römpp, A.; Spengler, B.; Gottwald, S. Histology-guided high-resolution AP-SMALDI mass spectrometry imaging of wheat-Fusarium graminearum interaction at the root–shoot junction. *Plant Methods* **2018**, *14*, 103, doi:10.1186/s13007-018-0368-6.

10. Floyd, R.A.; West, M.S.; Hogsett, W.E.; Tingey, D.T. Increased 8-Hydroxyguanine Content of Chloroplast DNA from Ozone-Treated Plants. *Plant Physiol.* **1989**, *91*, doi:10.1104/pp.91.2.644.

11. Perochon, A.; Benbow, H.R.; Ślęczka-Brady, K.; Malla, K.B.; Doohan, F.M. Analysis of the chromosomal clustering of Fusarium-responsive wheat genes uncovers new players in the defence against head blight disease. *Sci. Rep.* **2021**, *11*, doi:10.1038/s41598-021-86362-4.

12. Chetal, S.; Wagle, D.S.; Nainawatee, H.S. Glycolipid changes in wheat and barley chloroplast under water stress. *Plant Sci. Lett.* **1981**, *20*, doi:10.1016/0304-4211(81)90266-2.